Constraints on effective field theory parameters for the $\Lambda N \to NN$ transition

Axel Pérez-Obiol,[1,*] Assumpta Parreño,[1,†] and Bruno Juliá-Díaz[1,2,‡]

[1]*Departament d'Estructura i Constituents de la Matèria, Institut de Ciències del Cosmos (ICC), Universitat de Barcelona, Martí i Franquès 1, E–08028, Spain*

[2]*Institut de Ciències Fotòniques (ICFO), Parc Mediterrani de la Tecnologia, E-08860 Castelldefels (Barcelona), Spain*

(Received 25 April 2011; published 8 August 2011)

The relation between the low-energy constants appearing in the effective field theory description of the $\Lambda N \to NN$ transition potential and the parameters of the one-meson-exchange model previously developed is obtained. We extract the relative importance of the different exchange mechanisms included in the meson picture by means of a comparison to the corresponding operational structures appearing in the effective approach. The ability of this procedure to obtain the weak baryon-baryon-meson couplings for a possible scalar exchange is also discussed.

DOI: 10.1103/PhysRevC.84.024606 PACS number(s): 13.75.Ev, 21.80.+a, 25.80.Pw, 13.30.Eg

I. INTRODUCTION

The use of effective field theory (EFT) approaches provides a systematic way of handling nonperturbative strong interaction physics. In particular, it is appealing for the description of the short-distance physics of baryon-baryon interactions.

The EFT for the nonleptonic weak $|\Delta S| = 1 \Lambda N$ interaction, which is the main process responsible for the nonmesonic decay of mostly all hypernuclei was formulated in Refs. [1] and [2]. While the authors in [1] constructed the effective theory by adding to the long-range one-pion-exchange mechanism (OPE) a four-fermion-point interaction, coming from Lorentz four-vector currents, Ref. [2] added the K-exchange mechanism (OKE) to the intermediate range of the interaction, as well as additional operational structures to the short-range part of the transition potential. These structures result when all possible operators compatible with the symmetries fulfilled by the weak $|\Delta S| = 1$ ΛN interaction are considered. The local operators governing short distance dynamics in any EFT appear in the Lagrangian multiplied by low-energy constants (LECs), which have to be determined by a fit to the available experimental data. Although neither the amount nor the quality of hypernuclear weak decay data is comparable with the wealth of information available in the nonstrange sector, these data are enough to fairly constrain the lowest-order LECs. In order to provide a higher-order description of the weak four-fermion interaction, and therefore, a deeper understanding of the fundamental dynamics involved, more and better data are needed, or in their absence, a mapping to successful one-meson-exchange (OME) models can be performed. Understanding these low-energy constants in terms of physical ingredients of the OME models, as masses, strong form factor parameters and couplings of pseudoscalar and vector mesons to baryons, is called resonance saturation [3] and it is the aim of this paper.

The present work is partly motivated by the possible presence of an isoscalar spin-independent central-transition operator in the weak-decay mechanism, and its relevant role in the prediction of some hypernuclear decay observables [2,4,5]. This operational structure would map a scalar σ-meson resonance in the traditional meson-exchange picture. The fact that the σ does not belong to the ground-state meson octet has prevented its inclusion in many OME treatments of the weak transition amplitude. Some works, however, have included the phenomenological exchange of a correlated 2-π (and/or 2-ρ pair) state coupled to a scalar-isoscalar channel, understood as a σ resonance [6–9], and pointed out its relevance to determine the strength of some particular transition amplitudes. The publication of accurate data on hypernuclear decay observables during the last five years, makes it timely to revise the calculation of Ref. [2], and explore the feasibility of the EFT approach to constrain the weak baryon-baryon-sigma coupling constants.

To facilitate the reading of this paper, and although the EFT formalism as well as the OME one were developed and presented elsewhere, we choose to include here a schematic overview of basics, together with the final relations governing the weak dynamics according to each one of the approaches.

II. MESON EXCHANGE POTENTIAL

The Λ hyperon decays in free space through the nonleptonic weak decay modes $\Lambda \to n\pi^0$ and $\Lambda \to p\pi^-$, with an approximate ratio of 36:64. This mechanism is highly suppressed in the nuclear medium, since the momentum of the nucleon in the final state is not large enough to access unoccupied states above the Fermi energy level. However, hypernuclear systems decay, precisely due to the presence of surrounding nucleons, by means of single-nucleon-induced, $\Gamma_{1N} = \Lambda N \to NN$, and multinucleon-induced decay mechanisms. Recently, the detection of two nucleons in coincidence in the final state [10–12] has allowed a more reliable extraction not only of the total nonmesonic decay rate, but also of the ratio between the neutron-induced process ($\Lambda n \to nn$) and the proton-induced one ($\Lambda p \to np$), Γ_n/Γ_p [13,14]. The analysis

*axel@ecm.ub.es
†assum@ecm.ub.es
‡bruno@ecm.ub.es

of the data points out that, in order to isolate the physical region where medium effects and multinucleon-induced processes are minimal, one needs to study the energy and angular correlated spectra for the particles detected in the final state, instead of looking at the absolute values for the partial and total decay rates. Additionally, experiments performed with polarized hypernuclei provide us with a measure of the asymmetry in the angular distribution of protons in the final state, asymmetry that can be understood from the interference between the parity-conserving (PC) and parity-violating (PV) weak amplitudes. The explicit expressions for the different decay rates, as well as the PV asymmetry, can be found in the original reference [15].

Traditionally, and in analogy with the strong NN interaction, the one-nucleon-induced decay mode, $\Lambda N \to NN$, has been described by a one-boson-exchange model, according to which a pion emitted at the weak ΛN vertex is absorbed by the NN pair at the strong one. While mesons other than the pion would be forbidden for the decay of the Λ particle in free space, there is no restriction for the off-shell exchange of massive bosons. In the considered energy domain, one needs to explicitly consider the exchange of the ground state of pseudoscalar and vector meson octets. Higher energy physics is parameterized through explicit cutoffs of ≈ 1 GeV. The momentum space transition potential will be therefore given by the nonrelativistic limit of the appropriate Feynman amplitude depicted in Figs. 1(a) and 1(b).

Using the strong and weak Hamiltonians given explicitly in Appendix A, the OPE potential reads:

$$V_\pi(\vec{q}) = -G_F m_\pi^2 \frac{g}{2M_S}\left(\hat{A} + \frac{\hat{B}}{2M_W}\vec{\sigma}_1\vec{q}\right)\frac{\vec{\sigma}_2\vec{q}}{\vec{q}^{\,2}+\mu^2}, \qquad (2.1)$$

where $\vec{q} = \vec{p}_1 - \vec{p}_3$ is the momentum carried by the pion directed towards the strong vertex, $g = g_{NN\pi}$ the strong coupling constant for the $NN\pi$ vertex, μ the pion mass, M_S (M_W) the average of the baryon masses at the strong (weak) vertex, and $\hat{A} = A_\pi \vec{\tau}_1\vec{\tau}_2$ and $\hat{B} = B_\pi \vec{\tau}_1\vec{\tau}_2$ the isospin operators containing the weak parity-violating and parity-conserving coupling constants.

The η and K exchanges, whose strong and weak vertices are again explicitly given in Appendix A, can be obtained from Eq. (2.1) by making the replacements

$$g \to g_{NN\eta}, \quad \mu \to m_\eta, \quad \hat{A} \to A_\eta, \quad \hat{B} \to B_\eta$$

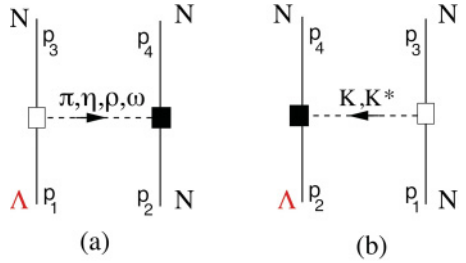

FIG. 1. (Color online) (a) Nonstrange and (b) strange meson-exchange contributions to the $\Lambda N \to NN$ weak transition potential. A weak insertion is indicated by an empty square, while a filled square stands for a strong interaction vertex.

in the case of the η exchange, and

$$\begin{aligned} g &\to g_{\Lambda NK}, \quad \mu \to m_K, \\ \hat{A} &\to \left(\frac{C_K^{PV}}{2} + D_K^{PV} + \frac{C_K^{PV}}{2}\vec{\tau}_1\vec{\tau}_2\right), \\ \hat{B} &\to \left(\frac{C_K^{PC}}{2} + D_K^{PC} + \frac{C_K^{PC}}{2}\vec{\tau}_1\vec{\tau}_2\right) \end{aligned} \qquad (2.2)$$

in the case of the K exchange.

The short-range one-meson exchange ΛN interaction is supplemented by the inclusion of more massive bosons, up to a mass of around 1 GeV, the ρ, ω, and K^* mesons. For the ρ meson, for example, the nonrelativistic reduction of the pertinent Feynman amplitude, computed using the vertices of Appendix A, gives the following transition potential:

$$\begin{aligned} V_\rho(\vec{q}) = \Bigg[& F_1\hat{\alpha} - \frac{(\hat{\alpha}+\hat{\beta})(F_1+F_2)}{4M_S M_W}(\vec{\sigma}_1\times\vec{q})(\vec{\sigma}_2\times\vec{q}) \\ & - \mathrm{i}\frac{\hat{\varepsilon}(F_1+F_2)}{2M_S}(\vec{\sigma}_1\times\vec{\sigma}_2)\vec{q}\Bigg]\frac{G_F m_\pi^2}{\vec{q}^{\,2}+\mu^2}, \end{aligned} \qquad (2.3)$$

with $\mu = m_\rho$, $F_1 = g^V_{NN\rho}$, $F_2 = g^T_{NN\rho}$ and where the operators $\hat{\alpha}$, $\hat{\beta}$, and $\hat{\varepsilon}$, defined by

$$\hat{\alpha} = \alpha_\rho \vec{\tau}_1\vec{\tau}_2, \quad \hat{\beta} = \beta_\rho \vec{\tau}_1\vec{\tau}_2, \quad \hat{\varepsilon} = \varepsilon_\rho \vec{\tau}_1\vec{\tau}_2,$$

contain the isospin structure in addition to the weak coupling constants.

The nonrelativistic potential can be obtained from the general expression given in Eq. (2.3) by making the following replacements:

$$\begin{aligned} &\mu \to m_\omega, \quad F_1 \to g^V_{NN\omega}, \quad F_2 \to g^T_{NN\omega}, \\ &\hat{\alpha} \to \alpha_\omega, \quad \hat{\beta} \to \beta_\omega, \quad \hat{\varepsilon} \to \varepsilon_\omega \end{aligned} \qquad (2.4)$$

in the case of the ω exchange, and

$$\begin{aligned} &\mu \to m_{K^*}, \quad F_1 \to g^V_{\Lambda NK^*}, \quad F_2 \to g^T_{\Lambda NK^*} \\ &\hat{\alpha} \to \frac{C_{K^*}^{PC,V}}{2} + D_{K^*}^{PC,V} + \frac{C_{K^*}^{PC,V}}{2}\vec{\tau}_1\vec{\tau}_2 \\ &\hat{\beta} \to \frac{C_{K^*}^{PC,T}}{2} + D_{K^*}^{PC,T} + \frac{C_{K^*}^{PC,T}}{2}\vec{\tau}_1\vec{\tau}_2 \\ &\hat{\varepsilon} \to \left(\frac{C_{K^*}^{PV}}{2} + D_{K^*}^{PV} + \frac{C_{K^*}^{PV}}{2}\vec{\tau}_1\vec{\tau}_2\right) \end{aligned} \qquad (2.5)$$

for the exchange of a K^* meson. Note that the K^* weak vertex has the same structure as the K one, the only difference being the parity-conserving contribution, which has two terms, related to the vector and tensor couplings.

Due to the lack of enough phase space to produce the desired decay vertex, the baryon-baryon-meson couplings for mesons heavier than the pion are not available experimentally. To fix such couplings one uses SU(3) flavor (SU(6) spin flavor) symmetry to relate the unknown couplings involving pseudoscalar (vector) mesons to the pionic decay vertex. For the strong vertices we use the values given by the Nijmegen soft-core f [16] and the Jülich B [17] models, which also rely on the same symmetries. This choice generates a model dependency in our approach, which also propagates to the weak couplings through the pole model [18] used to evaluate the weak PC

TABLE I. Nijmegen (NSC97f) meson-exchange parameters used in the present work. The weak couplings are in units of $G_F m_\pi{}^2 = 2.21 \times 10^{-7}$.

M	Strong c.c.	Weak c.c.		Λ_i
		PC	PV	(GeV)
π	$g_{NN\pi} = 13.16$	$B_\pi = -7.15$	$A_\pi = 1.05$	1.750
η	$g_{NN\eta} = 6.42$	$B_\eta = -11.9$	$A_\eta = 1.80$	1.750
K	$g_{\Lambda NK} = -17.66$	$C_K^{PC} = -23.70$	$C_K^{PV} = 0.76$	1.789
	$g_{N\Sigma K} = 5.38$	$D_K^{PC} = 8.33$	$D_K^{PV} = 2.09$	
ρ	$g^V_{NN\rho} = 2.97$	$\alpha_\rho = -3.29$	$\epsilon_\rho = 1.09$	1.232
	$g^T_{NN\rho} = 12.52$	$\beta_\rho = -6.74$		
ω	$g^V_{NN\omega} = 10.36$	$\alpha_\omega = -0.17$	$\epsilon_\omega = -1.33$	1.310
	$g^T_{NN\omega} = 4.195$	$\beta_\omega = -7.43$		
K^*	$g^V_{\Lambda NK^*} = -6.105$	$C^{PC,V}_{K^*} = -4.02$	$C^{PV}_{K^*} = -4.48$	1.649
	$g^T_{\Lambda NK^*} = -14.85$	$C^{PC,T}_{K^*} = -19.54$		
		$D^{PC,V}_{K^*} = -5.46$	$D^{PV}_{K^*} = 0.60$	
		$D^{PC,T}_{K^*} = 6.23$		

baryon-baryon-meson constants. In order to be consistent, we use the same strong potential models to derive the scattering (T matrix) NN wave functions in the final state [19].

To regularize the potentials at higher energies we include a form factor at each vertex of the OME diagram. The form of this form factor depends on the strong interaction model we are considering. In the case of the Jülich B model we use a monopole form factor, $F(\vec{q}) = (\Lambda_i^2 - \mu_i^2)/(\Lambda_i^2 + \vec{q}^2)$, at each vertex, while for the Nijmegen SC97 models, we use a modified monopole version [19], $F(\vec{q}) = \Lambda_i^2/(\Lambda_i^2 + \vec{q}^2)$. In both cases, the value of the cutoff, Λ_i, depends on the meson exchanged (with mass μ_i). The full set of meson-exchange parameters employed here is given in Tables I and II.

III. EFFECTIVE FIELD THEORY APPROACH

To a given order in the EFT approach, the weak nonleptonic $\Lambda N \to NN$ interaction is built by adding to the π and K exchange mechanisms a series of local terms with increasing dimension (i.e., increasing number of derivatives) and

TABLE II. Same as Table I but for the Jülich B model.

M	Strong c.c.	Weak c.c.		Λ_i
		PC	PV	(GeV)
π	$g_{NN\pi} = 13.45$	$B_\pi = -7.15$	$A_\pi = 1.05$	1.300
η	$g_{NN\eta} = 0$	$B_\eta = 0$	$A_\eta = 1.80$	1.300
K	$g_{\Lambda NK} = -13.48$	$C_K^{PC} = -17.67$	$C_K^{PV} = 0.76$	1.200
	$g_{N\Sigma K} = 3.55$	$D_K^{PC} = 5.50$	$D_K^{PV} = 2.09$	
ρ	$g^V_{NN\rho} = 3.25$	$\alpha_\rho = -3.60$	$\epsilon_\rho = 1.09$	1.400
	$g^T_{NN\rho} = 19.82$	$\beta_\rho = -9.55$		
ω	$g^V_{NN\omega} = 15.85$	$\alpha_\omega = -5.85$	$\epsilon_\omega = -1.33$	1.500
	$g^T_{NN\omega} = 0$	$\beta_\omega = -10.96$		
K*	$g^V_{\Lambda NK^*} = -5.63$	$C^{PC,V}_{K^*} = -3.71$	$C^{PV}_{K^*} = -4.48$	2.200
	$g^T_{\Lambda NK^*} = -18.34$	$C^{PC,T}_{K^*} = -26.38$		
		$D^{PC,V}_{K^*} = -5.03$	$D^{PV}_{K^*} = 0.60$	
		$D^{PC,T}_{K^*} = 12.18$		

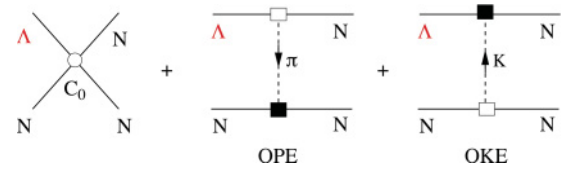

FIG. 2. (Color online) Lowest-order contribution to the weak $\Lambda N \to NN$ diagram. Empty symbols represent weak vertices while solid ones represent strong vertices. A circle stands for a nonderivative operator.

compatible with chiral symmetry, Lorentz invariance, and the applicable discrete symmetries.

Therefore, the leading-order (LO) contribution will contain, apart from the OPE and OKE diagrams, contact operators with no derivatives acting on the four-baryon vertex. The inclusion of the long-range π-exchange mechanism is justified by the high value of the momentum transfer in the weak reaction, $|\vec{q}| \sim 400$ MeV, a consequence of the difference between the Λ and nucleon masses in the initial state. The same argument holds for the explicit inclusion of the K meson, supported also by chiral symmetry. From the diagramatical point of view the LO contribution to the potential is given by Fig. 2.

One may, equivalently, proceed to chirally expand the vertices entering the $\Lambda N \to NN$ transition, and use a phenomenological approach to account for the strong interaction between the baryons involved in the process. Those vertices are nothing else but combinations of the five Dirac bilinear covariants: $1, \gamma^5, \gamma^\mu, \gamma^\mu\gamma^5$, and $\frac{i\sigma^{\mu\nu}q_\nu}{2M}$, where $\sigma^{\mu\nu} = \frac{i}{2}[\gamma^\mu, \gamma^\nu]$, M is the mass of the baryon, and q_ν is the transferred momentum. Since the relativistic form of these bilinears encodes all the orders in a momentum expansion, it is their chiral expansion that will better allow the power counting by comparing nonrelativistic terms of size 1, p/M, etc. In order to avoid formal inconsistencies from the chiral point of view, we rely directly on the terms that enter at each order given the symmetries fulfilled by the weak $|\Delta S| = 1$ transition.

All these possible transitions are shown in Table III for an initial S-wave ΛN state, where the model-independent leading-order operators in momentum space responsible for the transitions are listed (we are assuming that $|\vec{p}_1 - \vec{p}_2|$ is small enough to disregard higher powers of the derivative operators $\vec{p}_1 - \vec{p}_2$). Organizing all these contributions in increasing size operators, we obtain the most general Lorentz invariant potential, with no derivatives in the fields, for the four-fermion (4P) interaction in momentum space up to

TABLE III. $\Lambda N \to NN$ transitions for an initial ΛN relative S-wave state.

partial wave	operator	size	I
$a: {}^1S_0 \to {}^1S_0$	$\hat{1}, \vec{\sigma}_1\vec{\sigma}_2$	1	1
$b: {}^1S_0 \to {}^3P_0$	$(\vec{\sigma}_1 - \vec{\sigma}_2)\vec{q}, (\vec{\sigma}_1 \times \vec{\sigma}_2)\vec{q}$	q/M_N	1
$c: {}^3S_1 \to {}^3S_1$	$\hat{1}, \vec{\sigma}_1\vec{\sigma}_2$	1	0
$d: {}^3S_1 \to {}^1P_1$	$(\vec{\sigma}_1 - \vec{\sigma}_2)\vec{q}, (\vec{\sigma}_1 \times \vec{\sigma}_2)\vec{q}$	q/M_N	0
$e: {}^3S_1 \to {}^3P_1$	$(\vec{\sigma}_1 + \vec{\sigma}_2)\vec{q}$	q/M_N	1
$f: {}^3S_1 \to {}^3D_1$	$(\vec{\sigma}_1 \times \vec{q})(\vec{\sigma}_2 \times \vec{q})$	$q^2/M_N{}^2$	0

$\mathcal{O}(q^2/M^2)$ order (in units of $G_F = 1.166 \times 10^{-11}$ MeV^{-2})

$$V_{4P}(\vec{q}) = C_0^0 + C_0^1\,\vec{\sigma}_1\vec{\sigma}_2 + C_1^0\,\frac{\vec{\sigma}_1\vec{q}}{2\overline{M}} + C_1^1\,\frac{\vec{\sigma}_2\vec{q}}{2M} + iC_1^2\,\frac{(\vec{\sigma}_1\times\vec{\sigma}_2)\,\vec{q}}{2\tilde{M}} + C_2^0\,\frac{\vec{\sigma}_1\vec{q}\;\vec{\sigma}_2\vec{q}}{4M\overline{M}} + C_2^1\,\frac{\vec{\sigma}_1\vec{\sigma}_2\,\vec{q}^{\,2}}{4M\overline{M}} + C_2^2\,\frac{\vec{q}^2}{4M\tilde{M}}, \tag{3.1}$$

where M is the nucleon mass, $\overline{M} = (M + M_\Lambda)/2$, $\tilde{M} = (3M + M_\Lambda)/4$ (with M_Λ the Λ mass), and C_i^j is the jth low energy coefficient at ith order. To derive the previous expression, we have used the relation $(\vec{\sigma}_1\times\vec{q})(\vec{\sigma}_2\times\vec{q}) = (\vec{\sigma}_1\vec{\sigma}_2)\,\vec{q}^{\,2} - (\vec{\sigma}_1\vec{q})(\vec{\sigma}_2\vec{q})$. Notice that, in principle, one could write, at next-to-next-to-leading-order (NNLO) another set of eight operators containing the isospin structure $\vec{\tau}_1\vec{\tau}_2$. However, once one imposes that the final two-nucleon state must be antisymmetric, the number of structures in the effective potential is reduced to half the original, leaving to only eight independent operators.

The relation between the LO constants appearing in Eq. (3.1) and the ones in the nonantisymmetrized potential,

$$V_{4P}^{LO'}(\vec{q}) = C_{0sc}^0 + C_{0vec}^0\;\vec{\tau}_1\vec{\tau}_2 + C_{0sc}^1\vec{\sigma}_1\vec{\sigma}_2 + C_{0vec}^1\vec{\sigma}_1\vec{\sigma}_2\;\vec{\tau}_1\vec{\tau}_2$$

is the following (see Ref. [20]):

$$\begin{aligned} C_0^0 &= C_{0sc}^0 - 2\,C_{0vec}^0 - 3C_{0vec}^1 \\ C_0^1 &= C_{0sc}^1 - C_{0vec}^0. \end{aligned} \tag{3.2}$$

From the former derivation, it is clear that the form of the contact terms is model independent. The LECs represent the short-distance contributions and their size depends on how the theory is formulated, and more specifically upon the chiral order we are working with. The low-energy parameters are fitted to the known weak-decay observables discussed in Sec. II.

IV. RELATIONS BETWEEN ONE-MESON EXCHANGE POTENTIALS AND THE EFFECTIVE FIELD THEORY

To relate the meson-exchange constants to the LECs in the effective $\Lambda N \to NN$ potential, we perform a low-momentum expansion of the various (regularized) meson-exchange potentials other than the pion and the kaon, since these two are explicitly included in both the OME and the EFT approaches. This procedure leads to a series of contact terms organized by their increasing dimension (i.e., with increasing powers of momenta), an appropriate form to compare with the EFT potential. Therefore, one can write these terms up to $\mathcal{O}(\vec{q}^2/M^2)$ order (in units of $G_F = 1.166 \times 10^{-11}$ MeV^{-2}) as

$$\begin{aligned}
V_{OME}^{LO}(\vec{q}) &= \left[\frac{g^V_{\Lambda NK^*}}{{m_{K^*}}^2}\left(\frac{C^{PC,V}_{K^*}}{2} + D^{PC,V}_{K^*}\right) + \frac{g^V_{NN\omega}\alpha_\omega}{{m_\omega}^2} + \left(\frac{g^V_{\Lambda NK^*}C^{PC,V}_{K^*}}{2{m_{K^*}}^2} + \frac{g^V_{NN\rho}\alpha_\rho}{{m_\rho}^2}\right)\vec{\tau}_1\vec{\tau}_2\right]{m_\pi}^2, \\
V_{OME}^{NLO}(\vec{q}) &= \frac{-{m_\pi}^2}{2M}\frac{A_\eta g_{NN\eta}}{{m_\eta}^2}\vec{\sigma}_2\vec{q} - \frac{{m_\pi}^2}{2M}\left[\left(\frac{i\left(g^V_{\Lambda NK^*} + g^T_{\Lambda NK^*}\right)\left(\frac{C^{PV}_{K^*}}{2} + D^{PV}_{K^*}\right){m_\pi}^2}{{m_{K^*}}^2} + \frac{i\left(g^V_{NN\omega} + g^T_{NN\omega}\right)\epsilon_\omega{m_\pi}^2}{{m_\omega}^2}\right)\right. \\
&\quad \left. + \left(\frac{i\left(g^V_{\Lambda NK^*} + g^T_{\Lambda NK^*}\right)C^{PV}_{K^*}{m_\pi}^2}{2{m_{K^*}}^2} + \frac{i\left(g^V_{NN\rho} + g^T_{NN\rho}\right)\epsilon_\rho{m_\pi}^2}{{m_\rho}^2}\right)\vec{\tau}_1\vec{\tau}_2\right](\vec{\sigma}_1\times\vec{\sigma}_2)\vec{q}, \\
V_{OME}^{NNLO}(\vec{q}) &= \frac{{m_\pi}^2}{4M\overline{M}}\left[\left(\frac{C^{PC,V}_{K^*}}{2} + D^{PC,V}_{K^*} + \frac{C^{PC,T}_{K^*}}{2} + D^{PC,T}_{K^*}\right)\frac{g^V_{\Lambda NK^*} + g^T_{\Lambda NK^*}}{{m_{K*}}^2} + \frac{(\alpha_\omega + \beta_\omega)\left(g^V_{NN\omega} + g^T_{NN\omega}\right)}{{m_\omega}^2}\right. \\
&\quad \left. + \left(\frac{\left(C^{PC,V}_{K^*} + C^{PC,T}_{K^*}\right)\left(g^V_{\Lambda NK^*} + g^T_{\Lambda NK^*}\right)}{2{m_{K*}}^2} + \frac{(\alpha_\rho + \beta_\rho)(g^V_{NN\rho} + g^T_{NN\rho})}{{m_\rho}^2}\right)\vec{\tau}_1\vec{\tau}_2\right](\vec{\sigma}_1\vec{q}\vec{\sigma}_2\vec{q} - \vec{\sigma}_1\vec{\sigma}_2\vec{q}^2) \\
&\quad - \frac{{m_\pi}^2}{4M\overline{M}}\frac{B_\eta g_{NN\eta}}{{m_\eta}^2}\vec{\sigma}_1\vec{q}\vec{\sigma}_2\vec{q} - 2{m_\pi}^2\left[\frac{g^V_{\Lambda NK^*}(\Lambda^2 + {m_{K^*}}^2)\left(\frac{C^{PC,V}_{K^*}}{2} + D^{PC,V}_{K^*}\right)}{{m_{K^*}}^4\Lambda^2} + \frac{g^V_{NN\omega}\alpha_\omega(\Lambda^2 + {m_\omega}^2)}{{m_\omega}^4\Lambda^4}\right. \\
&\quad \left. + \left(\frac{g^V_{\Lambda NK^*}(\Lambda^2 + {m_{K^*}}^2)C^{PC,V}_{K^*}}{2{m_{K^*}}^4\Lambda^2} + \frac{g^V_{NN\rho}\alpha_\rho(\Lambda^2 + {m_\rho}^2)}{{m_\rho}^4\Lambda^4}\right)\vec{\tau}_1\vec{\tau}_2\right]\vec{q}^2.
\end{aligned} \tag{4.1}$$

We have chosen to show the explicit expressions of the LECs in terms of meson-exchange parameters in Appendix B. Here we only quote the relations at LO. In order to compare these expressions with the 4P potential of Eq. (3.1) we need to use the same base of operators. Eq. (3.2) allows us to obtain the LO coefficients in the $\hat{1}$, $\vec{\sigma}_1\vec{\sigma}_2$

TABLE IV. Values for the LECs obtained from the two sources: OME expansion and LO (PC) EFT calculation, using the Nijmegen and Jülich strong interaction models. All the quantities are in units of $G_F = 1.166 \times 10^{-11}$ MeV^{-2}.

	Nijmegen			Jülich		
	OME expansion	LO PC calculation		OME expansion	LO PC calculation	
C_0^0	1.07 ± 0.88	-0.92 ± 0.31	4.01 ± 0.23	-1.7 ± 2.6	4.03 ± 0.50	0.89 ± 0.58
C_0^1	0.02 ± 0.36	-2.41 ± 0.11	0.02 ± 0.33	0.12 ± 0.37	-0.30 ± 0.28	-1.52 ± 0.18
χ^2		3.89	13.43		4.26	4.58

base,

$$C_0^0 = \left[\frac{g^V_{\Lambda NK^*}}{{m_{K^*}}^2}\left(\frac{C^{PC,V}_{K^*}}{2} + D^{PC,V}_{K^*}\right) + \frac{g^V_{NN\omega}\alpha_\omega}{{m_\omega}^2} - \frac{g^V_{\Lambda NK^*}C^{PC,V}_{K^*}}{{m_{K^*}}^2} - \frac{2g^V_{NN\rho}\alpha_\rho}{{m_\rho}^2}\right]{m_\pi}^2, \tag{4.2}$$

$$C_0^1 = \left[-\frac{g^V_{\Lambda NK^*}C^{PC,V}_{K^*}}{2{m_{K^*}}^2} - \frac{g^V_{NN\rho}\alpha_\rho}{{m_\rho}^2}\right]{m_\pi}^2. \tag{4.3}$$

In Table IV we show the results for the LECs obtained within both formalisms. On the one hand, we quote the values for the coefficients obtained from Eqs. (4.2) and (4.3) (left column, under the label: OME expansion). The numerical values for the constants in front of the spin-isospin operators have been obtained for each strong interaction model, and Eq. (3.2) has been used to write the LECs in the antisymmetric base of operators. On the other hand, we show the values obtained from a fit of our EFT to reproduce the experimental data described in Sec. II (right column, under the label: LO calculation). We note that it is enough to consider the LO EFT (i.e., just two constants) to obtain a reasonable fit to the data. Notice that the values derived from the OME approach do not arise from any fit to the observables but from symmetry considerations together with studies of the strong baryon-baryon interaction. Their errors are estimated considering an uncertainty in the couplings of ±30%.

The fits give two minima for each one of the strong interaction models. Note that the two models differ not only on the kaon exchange contribution (coupling constants and cutoffs), but also on the final NN wave functions. The corresponding total χ^2 for a fit to 11 observables is also given in the table. In Fig. 3 we show the values for the observables used in the present fit together with their respective fitted values, while Fig. 4 shows the contribution of each point to the χ^2.

The results in Table IV show two important features. First, the LECs derived from the two OME models considered, Jülich and Nijmegen, are compatible albeit mostly due to the large theoretical uncertainties. The OME prediction for C_0^1 is in both cases compatible with zero. Secondly, the comparison between the OME extracted LECs' values and the LO PC fitted ones shows only partial agreement. The largest disagreement is seen in C_0^0 in all cases. In the next section we will discuss how this disagreement can be reduced with the inclusion of a scalar exchange in the OME formalism.

Note that the results for the LECs presented here are different from the ones given in Ref. [2]. This comparison has to be made with the results obtained with the Nijmegen NSC97f strong interaction model, which is the only one used in [2]. Apart from small (kinematical) changes in the final NN-wave functions, and in the regularization of the OKE mechanism, the main difference between both calculations

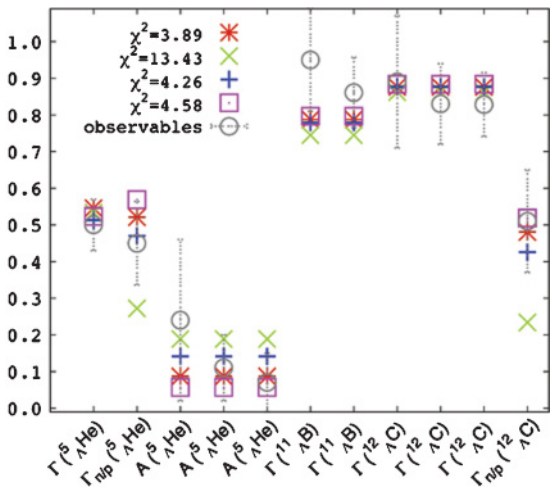

FIG. 3. (Color online) Hypernuclear decay observables (total and partial decay rates and asymmetry for ${}^{\Lambda}_{5}$He, ${}^{\Lambda}_{11}$B and ${}^{\Lambda}_{12}$C), including their error bars and their fitted values. The total decay rates are in units of the Λ decay rate in free space ($\Gamma_\Lambda = 3.8 \times 10^9 \text{s}^{-1}$). All the quantities are adimensional.

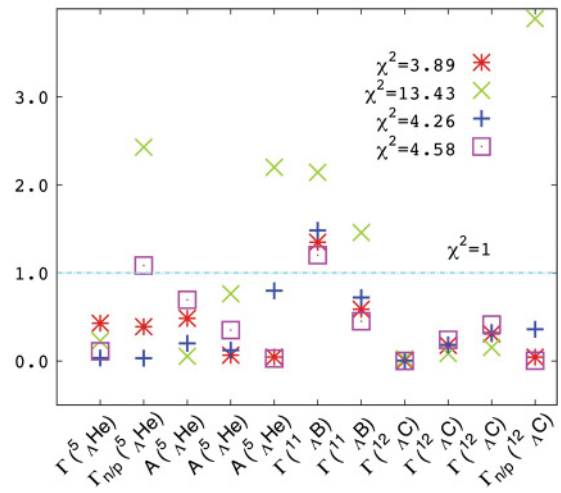

FIG. 4. (Color online) Contribution of each experimental point included in the fit to the total χ^2 for the four different fits discussed in the text.

resides in the experimental values used to perform the fit. We have updated our data set in order to include the recent rates extracted from the measure in coincidence of the two nucleons in the final state. Moreover, values of the neutron-to-proton (Γ_n/Γ_p) ratio close to one have been disregarded, following the last experimental and theoretical analysis, and more accurate data with smaller error bars have been included.

V. SCALAR EXCHANGE INTERACTION

By inspecting Table IV one clearly sees that the largest discrepancy affects the C_0^0 coefficient. This could be an indication of the relevance of a scalar exchange (σ), which is not explicitly included in the meson exchange formalism employed. A sensible way of inferring qualitatively the physical properties of such scalar would be to add it to the meson exchange description. The one-scalar-exchange (OSE) contribution can be obtained from the following weak and strong vertices [4]:

$$\begin{aligned}\mathcal{H}^{S}_{NN\sigma} &= g_{NN\sigma}\overline{\psi}_N\phi^\sigma\psi_N,\\ \mathcal{H}^{W}_{\Lambda N\sigma} &= G_F m_\pi^2\overline{\psi}_N\left(A_\sigma + B_\sigma\gamma_5\right)\phi^\sigma\psi_\Lambda\begin{pmatrix}0\\1\end{pmatrix},\end{aligned} \tag{5.1}$$

where A_σ and B_σ parametrize the parity-conserving and parity-violating weak amplitudes. In the nonrelativistic approximation, the corresponding potential reads,

$$V_{OSE}(\vec{q}) = -G_F m_\pi^2 g_{NN\sigma}\left(A_\sigma + \frac{B_\sigma}{2M_W}\vec{\sigma}_1\vec{q}\right)\frac{1}{\vec{q}^{\,2}+m_\sigma^2}. \tag{5.2}$$

We can now try to establish the values of the weak couplings A_σ and B_σ by direct comparison to the results of the fits. We can obtain information about A_σ using the numbers obtained in our LO (parity-conserving) fit. Insight on B_σ would require a NLO fit, which, as we already mentioned, is not needed to get a reasonable fit to our observables.

The OSE gives contribution, in particular, to C_0^0, which now becomes

$$\begin{aligned}C_0^{0(\sigma)} = \Bigg[&\frac{g^V_{\Lambda NK^*}}{m_{K^*}{}^2}\left(\frac{C^{PC,V}_{K^*}}{2}+D^{PC,V}_{K^*}\right)+\frac{g^V_{NN\omega}\alpha_\omega}{m_\omega{}^2}\\ &-\frac{g^V_{\Lambda NK^*}C^{PC,V}_{K^*}}{m_{K^*}{}^2}-\frac{2g^V_{NN\rho}\alpha_\rho}{m_\rho{}^2}-\frac{A_\sigma g_{NN\sigma}}{m_\sigma^2}\Bigg]m_\pi{}^2.\end{aligned} \tag{5.3}$$

Since C_0^1 is not modified by the inclusion of the σ, the minima that may be improved via this mechanism are the ones in which this coefficient is already in agreement with the one obtained from the OME expansion. Focusing on these minima (the ones with $\chi^2 = 13.43$ and $\chi^2 = 4.26$), we can extract the value of A_σ needed to make the two formalisms agree (at LO) within each strong interaction model. Using $m_\sigma = 550$ MeV and $g_{NN\sigma} = 8.8$ [21] we get values for A_σ in the range $3.3 \to 7.3$ for the Nijmegen minimum and in the range $4.8 \to 16$ for the Jülich one.

The shaded (blue) band in Figs. 5 and 6 shows the value of $C_0^{0(\sigma)}$ given by Eq. (5.3) as a function of A_σ, when the Nijmegen or Jülich strong interaction model is used respectively. Note that the error band in $C_0^{0(\sigma)}$ is given by the propagation of the uncertainties in the baryon-baryon-meson coupling constants, taken to be of the order of 30%. In the same plot we represent the corresponding fitted value in the EFT approach (solid orange) band. The range for A_σ quoted before corresponds to the intersection of both bands in the plot (i.e, the values for A_σ that make compatible the OME and EFT formalisms).

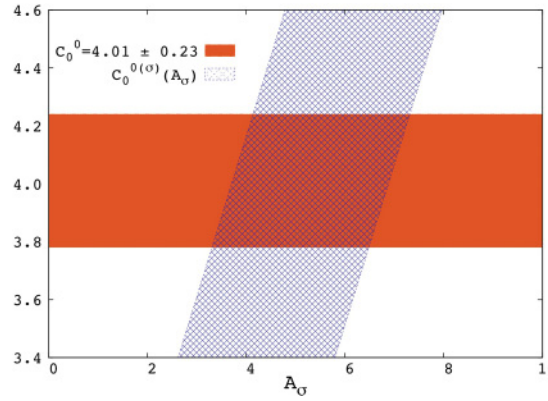

FIG. 5. (Color online) Comparison between C_0^0 and $C_0^{0(\sigma)}$ for the Nijmegen minimum. The shaded blue area represents the dependence of $C_0^{0(\sigma)}$ on A_σ given by Eq. (5.3), while the fitted EFT C_0^0 value is represented by the solid orange area. See text for details.

Other works have fitted this same parameter using different approaches. For instance, Ref. [4], which incorporates the OPE, OKE, and OSE mechanisms together with a direct-quark transition, uses the phenomenological approach of Block and Dalitz [22] to write the nonmesonic decay rates in terms of the squares of the amplitudes given in Table III for the s-shell ${}^{5}_{\Lambda}$He, ${}^{4}_{\Lambda}$He, and ${}^{4}_{\Lambda}$H hypernuclei. This factorization in terms of two-body amplitudes is possible when effective (spin-independent) correlations are used to account for the strong interaction among baryons, where no mixing between the different partial waves is possible. The strong interaction model used in this work is NSC97f. This approach leads to a quadratic equation to determine the couplings, resulting in two values for A_σ, 3.9 and -1.0 (note that the first of these two values is compatible with the range we are quoting for this constant when the same strong interaction model is used). Another approach was followed in Ref. [5], where the exchanges of all the mesons belonging to the pseudoscalar and vector mesons octets are

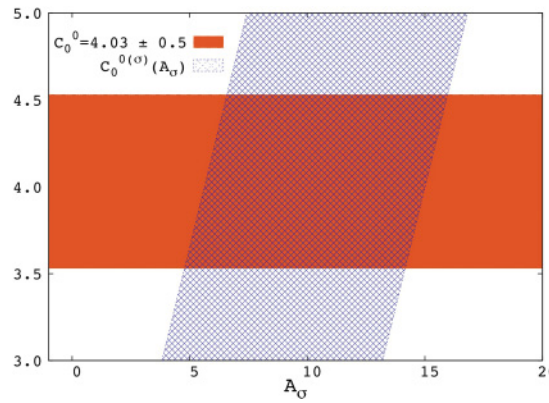

FIG. 6. (Color online) Same as Fig. 5 but for the Jülich minimum.

considered in the weak transition in addition to the σ meson, while again, effective (spin-independent) correlations are used in the strong sector. Fixing the value of the strong $NN\sigma$ coupling to be the same as the πNN one, a range of variation for the σ mass and cutoff leads to different values for the weak couplings, once a fit to the nonmesonic decay rate and the neutron-to-proton ratio for ${}^{5}_{\Lambda}$He is performed. Even though the inclusion of the σ-exchange mechanism does modify their prediction for the intrinsic asymmetry, their results are insensitive to the particular values of the A_σ and B_σ couplings, and a simultaneous reproduction of all the data is not achieved.

VI. CONCLUSION

We have derived the relations between the low-energy coefficients appearing in the EFT description of the two-body $\Lambda N \to NN$ transition driving the decay of hypernuclei and the parameters appearing in the widely used meson-exchange model. This has been achieved by comparing the momentum space expansion of the OME potentials to the different orders in the EFT formalism.

In both approaches, the one-pion- and one-kaon-exchange mechanisms are explicitly included to account for the long and intermediate ranges of the interaction. The higher mass contributions (η, ρ, ω, and K^*) in the OME model are parametrized as contact four-point interactions in the EFT approach. With this procedure we obtain relations for the LECs in terms of the masses, couplings, and cutoffs characteristic of the OME formalism. The numerical values for the LO EFT LECs have been obtained by fitting the available experimental data for hypernuclear decay observables. In the OME case, however, the LECs have been written in terms of the masses, couplings, and cutoffs, taken from their experimental values, symmetry constraints, or strong interaction models.

The considered experimental database of hypernuclear decay observables can be described with good accuracy within a LO EFT supplemented by π and K meson exchanges. This implies that further experimental efforts will be needed to constrain the higher-order terms in the EFT of hypernuclear decay.

Finally, we have analyzed the contribution of a scalar exchange in OME models, estimating the size of the corresponding parity conserving amplitude, needed to achieve a better agreement to the available experimental data.

ACKNOWLEDGMENTS

We thank Angels Ramos and Joan Soto for a careful reading of the manuscript.

This work was partly supported by MEC (Spain), Contract No. FIS2008-01661; FEDER, the EU Contract No. MRTN-CT-2006-035482, FLAVIAnet; MIUR, Contract No. 2001024324_007; the Generalitat de Catalunya, Contract No. 2005SGR-00343; and the European Community Research Infrastructure Integrating Activity *Study of Strongly Interacting Matter* (HadronPhysics2), Grant No, 227431, under the 7th Framework Program of the EU. A.P.-O. acknowledges support by the APIF PhD program of the University of Barcelona.

APPENDIX A: MESON-EXCHANGE POTENTIALS

The weak and strong vertices entering the one-pion-exchange (OPE) amplitude are

$$\begin{aligned}\mathcal{H}^{W}_{\Lambda N\pi} &= i G_F m_\pi^2 \overline{\psi}_N (A_\pi + B_\pi \gamma_5)\vec{\tau}\vec{\phi}^\pi \psi_\Lambda \begin{pmatrix}0\\1\end{pmatrix},\\ \mathcal{H}^{S}_{NN\pi} &= i g_{NN\pi}\overline{\psi}_N \gamma_5 \vec{\tau}\vec{\phi}^\pi \psi_N,\end{aligned} \tag{A1}$$

where $G_F m_\pi^2 = 2.21 \times 10^{-7}$ is the weak coupling constant, and A_π and B_π, empirical constants adjusted to the observables of the free Λ decay, which determine the strength of the parity-violating and parity-conserving amplitudes, respectively. The nucleon, Λ, and pion fields are given by ψ_N, ψ_Λ, and $\vec{\phi}^\pi$, respectively, while the isospin spurion $\binom{0}{1}$ is included to enforce the empirical $\Delta T = 1/2$ rule observed in the decay of a free Λ. The Bjorken and Drell convention for the definition of γ_5 [23] is taken.

For the exchange of the pseudoscalar η and K mesons, the strong and weak vertices are (weak constants are given in units of $G_F m_\pi^2$)

$$\begin{aligned}\mathcal{H}^{S}_{NN\eta} &= i g_{NN\eta}\overline{\psi}_N \gamma_5 \phi^\eta \psi_N,\\ \mathcal{H}^{W}_{\Lambda N\eta} &= i\overline{\psi}_N (A_\eta + B_\eta\gamma_5)\phi^\eta \psi_\Lambda \begin{pmatrix}0\\1\end{pmatrix},\\ \mathcal{H}^{S}_{\Lambda NK} &= i g_{\Lambda NK}\overline{\psi}_N \gamma_5 \phi^K \psi_\Lambda,\\ \mathcal{H}^{W}_{NNK} &= i\left[\overline{\psi}_N \begin{pmatrix}0\\1\end{pmatrix}\left(C_K^{PV} + C_K^{PC}\gamma_5\right)(\phi^K)^\dagger \psi_N\right.\\ &\quad \left. + \overline{\psi}_N \psi_N \left(D_K^{PV} + D_K^{PC}\gamma_5\right)(\phi^K)^\dagger \begin{pmatrix}0\\1\end{pmatrix}\right],\end{aligned} \tag{A2}$$

where the weak coupling constants cannot be taken directly from experiment.

The weak $\Lambda N\rho$, $\Lambda N\omega$, NNK^*, and strong $NN\rho$, $NN\omega$, ΛNK^* vertices are given by [24]

$$\mathcal{H}^{W}_{\Lambda N\rho} = \overline{\psi}_N \left(\alpha_\rho \gamma^\mu \quad - \beta_\rho i\frac{\sigma^{\mu\nu}q_\nu}{2\overline{M}} + \varepsilon_\rho \gamma^\mu\gamma_5\right)\vec{\tau}\vec{\rho}_\mu \psi_\Lambda \begin{pmatrix}0\\1\end{pmatrix}, \tag{A3}$$

$$\mathcal{H}^{S}_{NN\rho} = \overline{\psi}_N \left(g^V_{NN\rho}\gamma^\mu + i\frac{g^T_{NN\rho}}{2M}\sigma^{\mu\nu}q_\nu\right)\vec{\tau}\vec{\rho}_\mu \psi_N, \tag{A4}$$

$$\mathcal{H}^{S}_{NN\omega} = \overline{\psi}_N \left(g^V_{NN\omega}\gamma^\mu + i\frac{g^T_{NN\omega}}{2M}\sigma^{\mu\nu}q_\nu\right)\phi^\omega_\mu \psi_N \tag{A5}$$

$$\mathcal{H}^{W}_{\Lambda N\omega} = \overline{\psi}_N \left(\alpha_\omega \gamma^\mu \quad - \beta_\omega i\frac{\sigma^{\mu\nu}q_\nu}{2\overline{M}} + \varepsilon_\omega \gamma^\mu\gamma_5\right)\phi^\omega_\mu \psi_\Lambda \begin{pmatrix}0\\1\end{pmatrix}, \tag{A6}$$

$$\mathcal{H}^{S}_{\Lambda NK^*} = \overline{\psi}_N \left(g^V_{\Lambda NK^*}\gamma^\mu + i\frac{g^T_{\Lambda NK^*}}{2\overline{M}}\sigma^{\mu\nu}q_\nu\right)\phi^{K^*}_\mu \psi_\Lambda, \tag{A7}$$

$$\begin{aligned}\mathcal{H}^{W}_{NNK^*} &= \left[C^{PC,V}_{K^*}\overline{\psi}_N \begin{pmatrix}0\\1\end{pmatrix}\left(\phi^{K^*}_\mu\right)^\dagger \gamma^\mu \psi_N\right.\\ &\quad + D^{PC,V}_{K^*}\overline{\psi}_N \gamma^\mu \psi_N \left(\phi^{K^*}_\mu\right)^\dagger \begin{pmatrix}0\\1\end{pmatrix}\\ &\quad + C^{PC,T}_{K^*}\overline{\psi}_N \begin{pmatrix}0\\1\end{pmatrix}\left(\phi^{K^*}_\mu\right)^\dagger (-i)\frac{\sigma^{\mu\nu}q_\nu}{2M}\psi_N\\ &\quad + D^{PC,T}_{K^*}\overline{\psi}_N (-i)\frac{\sigma^{\mu\nu}q_\nu}{2M}\psi_N \left(\phi^{K^*}_\mu\right)^\dagger \begin{pmatrix}0\\1\end{pmatrix}\\ &\quad + C^{PV}_{K^*}\overline{\psi}_N \begin{pmatrix}0\\1\end{pmatrix}\left(\phi^{K^*}_\mu\right)^\dagger \gamma^\mu\gamma_5\psi_N\\ &\quad \left. + D^{PV}_{K^*}\overline{\psi}_N \gamma^\mu\gamma_5 \psi_N \left(\phi^{K^*}_\mu\right)^\dagger \begin{pmatrix}0\\1\end{pmatrix}\right].\end{aligned} \tag{A8}$$

APPENDIX B: LECS IN TERMS OF MESON-EXCHANGE PARAMETERS

The expressions for the LECs in terms of the meson-exchange parameters are the following:

$$C^0_{0sc} = \left[\frac{g^V_{\Lambda NK^*}}{{m_{K^*}}^2}\left(\frac{C^{PC,V}_{K^*}}{2} + D^{PC,V}_{K^*}\right) + \frac{g^V_{NN\omega}\alpha_\omega}{{m_\omega}^2}\right]{m_\pi}^2,$$

$$C^0_{0vec} = \left(\frac{g^V_{\Lambda NK^*}C^{PC,V}_{K^*}}{2{m_{K^*}}^2} + \frac{g^V_{NN\rho}\alpha_\rho}{{m_\rho}^2}\right){m_\pi}^2,$$

$$C^1_{0sc} = 0, \quad C^1_{0vec} = 0, \quad C^0_{1sc} = 0,$$

$$C^0_{1vec} = 0, \quad C^1_{1sc} = \frac{-{m_\pi}^2}{2M}\frac{A_\eta g_{NN\eta}}{{m_\eta}^2}, \quad C^1_{1vec} = 0, \tag{B1}$$

$$C^2_{1sc} = -\frac{{m_\pi}^2}{2M}\left[\frac{i\left(g^V_{\Lambda NK^*} + g^T_{\Lambda NK^*}\right)\left(\frac{C^{PV}_{K^*}}{2} + D^{PV}_{K^*}\right){m_\pi}^2}{{m_{K^*}}^2} + \frac{i\left(g^V_{NN\omega} + g^T_{NN\omega}\right)\epsilon_\omega {m_\pi}^2}{{m_\omega}^2}\right],$$

$$C^2_{1vec} = \frac{{m_\pi}^2}{2M}\left[\frac{i\left(g^V_{\Lambda NK^*} + g^T_{\Lambda NK^*}\right)C^{PV}_{K^*}{m_\pi}^2}{2{m_{K^*}}^2} + \frac{i\left(g^V_{NN\rho} + g^T_{NN\rho}\right)\epsilon_\rho {m_\pi}^2}{{m_\rho}^2}\right],$$

$$C^0_{2sc} = \frac{{m_\pi}^2}{4M\overline{M}}\left[\left(\frac{C^{PC,V}_{K^*}}{2} + D^{PC,V}_{K^*} + \frac{C^{PC,T}_{K^*}}{2} + D^{PC,T}_{K^*}\right)\frac{g^V_{\Lambda NK^*} + g^T_{\Lambda NK^*}}{{m_{K_*}}^2} + \frac{(\alpha_\omega + \beta_\omega)\left(g^V_{NN\omega} + g^T_{NN\omega}\right)}{{m_\omega}^2} - \frac{B_\eta g_{NN\eta}}{{m_\eta}^2}\right],$$

$$C^0_{2vec} = \frac{{m_\pi}^2}{4M\overline{M}}\left[\frac{\left(C^{PC,V}_{K^*} + C^{PC,T}_{K^*}\right)\left(g^V_{\Lambda NK^*} + g^T_{\Lambda NK^*}\right)}{2{m_{K_*}}^2} + \frac{(\alpha_\rho + \beta_\rho)\left(g^V_{NN\rho} + g^T_{NN\rho}\right)}{{m_\rho}^2}\right],$$

$$C^1_{2sc} = -\frac{{m_\pi}^2}{4M\overline{M}}\left[\left(\frac{C^{PC,V}_{K^*}}{2} + D^{PC,V}_{K^*} + \frac{C^{PC,T}_{K^*}}{2} + D^{PC,T}_{K^*}\right)\frac{g^V_{\Lambda NK^*} + g^T_{\Lambda NK^*}}{{m_{K_*}}^2} + \frac{(\alpha_\omega + \beta_\omega)\left(g^V_{NN\omega} + g^T_{NN\omega}\right)}{{m_\omega}^2}\right], \tag{B2}$$

$$C^1_{2vec} = -\frac{{m_\pi}^2}{4M\overline{M}}\left[\frac{\left(C^{PC,V}_{K^*} + C^{PC,T}_{K^*}\right)\left(g^V_{\Lambda NK^*} + g^T_{\Lambda NK^*}\right)}{2{m_{K_*}}^2} + \frac{(\alpha_\rho + \beta_\rho)\left(g^V_{NN\rho} + g^T_{NN\rho}\right)}{{m_\rho}^2}\right],$$

$$C^2_{2sc} = -2{m_\pi}^2\left[\frac{g^V_{\Lambda NK^*}\left(\Lambda^2 + {m_{K^*}}^2\right)\left(\frac{C^{PC,V}_{K^*}}{2} + D^{PC,V}_{K^*}\right)}{{m_{K^*}}^4\Lambda^2} + \frac{g^V_{NN\omega}\alpha_\omega\left(\Lambda^2 + {m_\omega}^2\right)}{{m_\omega}^4\Lambda^4}\right],$$

$$C^2_{2vec} = -2{m_\pi}^2\left[\frac{g^V_{\Lambda NK^*}\left(\Lambda^2 + {m_{K^*}}^2\right)C^{PC,V}_{K^*}}{2{m_{K^*}}^4\Lambda^2} + \frac{g^V_{NN\rho}\alpha_\rho\left(\Lambda^2 + {m_\rho}^2\right)}{{m_\rho}^4\Lambda^4}\right].$$

[1] Jung-Hwan Jun, Phys. Rev. C **63**, 044012 (2001).
[2] A. Parreño, C. Bennhold, and B. R. Holstein, Phys. Rev. C **70**, 051601 (2004); Nucl. Phys. A **754**, 127 (2005).
[3] G. Ecker, J. Kambor, and D. Wyler, Nucl. Phys. B **394**, 101 (1993).
[4] K. Sasaki, M. Izaki, and M. Oka, Phys. Rev. C **71**, 035502 (2005).
[5] C. Barbero and A. Mariano, Phys. Rev. C **73**, 024309 (2006).
[6] C. Chumillas, G. Garbarino, A. Parreño, and A. Ramos, Phys. Lett. B **657**, 180 (2007).
[7] K. Itonaga, T. Ueda, and T. Motoba, Nucl. Phys. A **585**, 331c (1995).
[8] E. Oset, D. Jido, and J. E. Palomar, Nucl. Phys. A **691**, 146 (2001).
[9] C. Barbero and A. Mariano, Phys. Rev. C **73**, 024309 (2006).
[10] H. Outa *et al.*, Nucl. Phys. A **754**, 157c (2005).
[11] B. H. Kang *et al.*, Phys. Rev. Lett. **96**, 062301 (2006).
[12] M. J. Kim *et al.*, Phys. Lett. B **641**, 28 (2006).
[13] G. Garbarino, A. Parreño, and A. Ramos, Phys. Rev. Lett. **91**, 112501 (2003).
[14] G. Garbarino, A. Parreño, and A. Ramos, Phys. Rev. C **69**, 054603 (2004).
[15] A. Parreño, A. Ramos, and C. Bennhold, Phys. Rev. C **56**, 339 (1997).
[16] V. G. J. Stoks and Th. A. Rijken, Phys. Rev. C **59**, 3009 (1999); Th. A. Rijken, V. G. J. Stoks, and Y. Yamamoto, *ibid.* **59**, 21 (1999).
[17] B. Holzenkamp, K. Holinde, and J. Speth, Nucl. Phys. A **500**, 485 (1989).

[18] J. F. Dubach, G. B. Feldman, B. R. Holstein, and L. de la Torre, Ann. Phys. (NY) **249**, 146 (1996).
[19] A. Parreño and A. Ramos, Phys. Rev. C **65**, 015204 (2001).
[20] E. Epelbaum, Ph.D. thesis, Ruhr-Universitat, 2000 (unpublished).
[21] R. Machleidt, Adv. Nucl. Phys. **19**, 189 (1989).
[22] M. M. Block and R. H. Dalitz, Phys. Rev. Lett. **11**, 96 (1963).
[23] J. D. Bjorken and S. D. Drell, *Relativistic Quantum Mechanics* (McGraw-Hill, New York, 1964).
[24] B. H. J. McKellar and B. F. Gibson, Phys. Rev. C **30**, 322 (1984).